Statistical Analysis of Nonparametric Transfer Function Estimates

Patrick Guillaume, *Member, IEEE,* István Kollár, and Rik Pintelon

***Abstract*—The Empirical Transfer Function Estimate (ETFE) is the ratio of the Fourier transforms of the output and input signals of a system. It works well when the input signal is deterministic and exactly known. However, when the input signal is random, or it can only be observed with an observation error, the quality of the ETFE deteriorates. Its variance can be *infinite* even for large signal-to-noise ratios. This is not well known.**

This paper establishes and analyzes a mathematical model of the ETFE with noisy input signals. It explains the cause of the large variance and suggests modifications which eliminate the above problems.

I. Introduction

ESTIMATION of the transfer function of a linear time-invariant system from measurements of its *input/output* (I/O) signals is important in a variety of engineering tasks and scientific investigations. If the I/O signals are deterministic and exactly known, the nonparametric estimate of the transfer function $G = G(\omega)$ at the angular frequency ω is the ratio of the output Fourier coefficient $V = V(\omega)$ and the input Fourier coefficient $U = U(\omega)$,

$$G(\omega) = \frac{V(\omega)}{U(\omega)}. \tag{1}$$

However, in practice, the input signal is often not known exactly, because it is measured with a certain observation noise (see Fig. 1). Therefore, the *true* I/O Fourier coefficients $\{U, V\}$ are not accessible, only $\{X, Y\}$ which are subject to some random perturbations $\{D, E\}$. The problem can be formulated using the following *errors-in-variables* (EV) model. Given

$$\begin{aligned} X &= U + D, \\ Y &= V + E \end{aligned} \tag{2}$$

determine the estimate of $G = V/U$.

Manuscript received December 20, 1995; revised January 29, 1996. This work was supported by the Belgian National Fund for Scientific Research (NFWO); the Flemish government (GOA-IMMI); the Belgian government as a part of the Belgian program on Inter-University Poles of Attraction (IUAP-50) initiated by the Belgian State, Prime Minister's Office, Science Policy Programming; the Fulbright Commission; and the U.S.-Hungarian Science and Technology Joint Fund, Project 299.

P. Guillaume and R. Pintelon are with the Department of Fundamental Electricity and Instrumentation, Vrije Universiteit Brussel, B-1050 Brussels, Belgium.

I. Kollár is with the Department of Measurement and Instrumentation Engineering, Technical University of Budapest, Hungary.

Publisher Item Identifier S 0018-9456(96)03518-8.

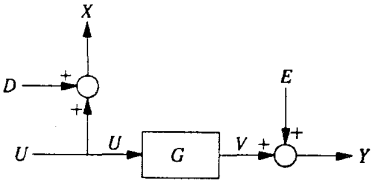

Fig. 1. Errors-in-variables setup.

Many papers have been devoted to the closely related topic of EV regression analysis [1]–[3]. Depending upon the nature of the *true* data U, i.e., whether it is random or deterministic, (2) is called in statistics a *structural relation* or a *functional relation,* respectively.

The classical approach to estimate the transfer function from noisy data is based on the so-called spectral estimators. In [5] alternative estimators based on nonlinear averaging techniques have been proposed for the functional relationship, providing smaller bias errors.

This paper investigates the variance of these nonparametric transfer function estimates. When an estimate depends nonlinearly on the observations, like the ratio on the denominator, the exact calculation of the variance can be very complicated, and approximations have to be used (see for instance [6, p. 151]). Linearization is often applied in system identification to derive the approximate bias and variance of an estimate (see e.g., [7, p. 167], and [8, p. 132]). These approximations are sometimes very poor. In the present paper we will investigate such cases and develop some improvements.

To pin-point what can go wrong with such approximations in a *functional relationship* (that is, for deterministic U), consider the *empirical transfer function estimator* (ETFE) in its elementary form, i.e., the ratio of two complex random variables

$$H = \frac{Y}{X} = \frac{V + E}{U + D}. \tag{3}$$

By linearizing (3) for $|D| \ll |U|$ and $|E| \ll |V|$,

$$H \approx G\left(1 - \frac{D}{U} + \frac{E}{V}\right) \tag{4}$$

and the variance of H is approximately

$$\operatorname{var}\{H\} \approx |G|^2 \left(\frac{\sigma_D^2}{|U|^2} + \frac{\sigma_E^2}{|V|^2}\right) \tag{5}$$

where σ_D^2 and σ_E^2 are the variances of the I/O disturbances. (For the sake of simplicity D and E are assumed to be uncorrelated.) However, for complex normally distributed Fourier coefficients [9] we will show that the exact variance (without linearization) is *infinite*! Furthermore, for a structural relationship with U itself complex normally distributed, Broersen [10] reported that the variance of the ETFE (3) is unbounded, *even when the true input U can be observed error-free (i.e., $D = 0$).*

The paper is organized as follows. In Section II the variance of the ETFE is determined. In Section III it is shown that by excluding a (small) region around the singularity point ($X = 0$) it is possible to obtain finite variances for the ETFE and similar 'infinite-variance' estimators. The impact of this modification on the bias is also examined. The variance of the logarithm of the ETFE is studied in Section IV. It turns out that the variance of $\ln(H)$ is *finite,* and the variance of the estimate of G, calculated from an average of $\ln(H)$ values, is also finite. In Section V, a general question is addressed: *What are the conditions on the measured data and on the estimator to obtain finite variances (and higher-order moments)?* Finally, the conclusions are drawn.

II. The Variance of the ETFE

An approximation of the variance of the ETFE is given by (5) for a functional relationship. When $\sigma_D^2 \ll |U|^2$ and $\sigma_E^2 \ll |V|^2$, Monte-Carlo simulations (e.g., with complex normally distributed I/O noise) seem to confirm the correctness of (5). However, it is shown in Appendix A for complex normally distributed errors with $\sigma_D^2 > 0$ and $U \neq 0$ that while the expected value of the estimate approximately equals the true value of G [5], the exact variance (without linearization) is *infinite*! The cause is that the noise on X can bring the denominator of (3) close to zero. This rarely happens for practical values of the input signal-to-noise ratio, which explains the Monte-Carlo results: the unlikely event usually does not happen even in a few thousand runs.

Even more surprising results can be obtained for the following nonparametric transfer function estimator,

$$\hat{H}_{\mathrm{EV}}^{[M]} = \frac{\frac{1}{M}\sum_{m=1}^{M} Y_m}{\frac{1}{M}\sum_{m=1}^{M} X_m} \tag{6}$$

where X_m and Y_m are given by an EV model

$$\left.\begin{aligned} X_m &= U + D_m \\ Y_m &= V + E_m \end{aligned}\right\} \qquad m = 1, \cdots, M. \tag{7}$$

So, X_m and Y_m are repeated observations of the same Fourier coefficients which are disturbed by additive complex noise. In practice, this means that a periodic excitation has to be used with $U \neq 0$ (i.e., a persistent excitation). Further, the excitation and the acquisition have to be synchroninized (i.e., one has to use the same sampling clock for both the generator and the acquisition). Furthermore, before starting the acquisition of the periodic excitation and response signals one has to wait until the initial transients died out.

If $\{X_m\}_{m=1}^{M}$ are independent and identically distributed and have finite mean U, then $\hat{X}_{\mathrm{EV}}^{[M]} = 1/M \ \Sigma_{m=1}^{M} X_m \to U$ with probability one. The proof is given in [11], pp. 290–292. The same theorem can be applied to the numerator of (6). Moreover, using the property that the almost sure limit of a continuous function equals the function of the almost sure limit, one obtains

$$\underset{M\to\infty}{\text{a.s.lim}}\ \hat{H}_{\mathrm{EV}}^{[M]} = \frac{\underset{M\to\infty}{\text{a.s.lim}}\ \hat{Y}_{\mathrm{EV}}^{[M]}}{\underset{M\to\infty}{\text{a.s.lim}}\ \hat{X}_{\mathrm{EV}}^{[M]}} = \frac{V}{U} = G. \tag{8}$$

When the data are independent and complex normally distributed ($D_m \in N_1^c(0, \sigma_D^2), E_m \in N_1^c(0, \sigma_E^2)$) the EV estimator reduces to a *maximum likelihood* (ML) estimator ([12], pp. 227–228). The Cramér-Rao lower bound is given by

$$\sigma_{\mathrm{CR}}^2 = \frac{|G|^2}{M}\left(\frac{\sigma_D^2}{|U|^2} + \frac{\sigma_E^2}{|V|^2}\right). \tag{9}$$

As the ML estimator is asymptotically efficient, the PDF of $\hat{H}_{\mathrm{EV}}^{[M]}$ converges for $M \to \infty$ to $N_1^c(G, \sigma_{\mathrm{CR}}^2)$ (i.e., convergence in law or in distribution). This limiting distribution has finite variance σ_{CR}^2. However, the variance is *infinite* for all finite values of M, so the variance itself does not converge to the Cramér-Rao lower bound. This example nicely illustrates that convergence in distribution does not imply convergence of the moments [13].

III. Exclusion of a Small Region Around the Singularity $X = 0$

The cause of the above discussed infinite variance is that the denominator can be arbitrarily small when the noise is close to $-U$. Therefore, it seems to be reasonable to 'robustify' the ETFE by excluding a small circle around the singularity $D/U = -1$ with radius ρ. This makes the variance finite, and causes a negligible bias only when ρ is small. The bias and variance of the transfer function estimate are functions of the radius ρ:

$$\mathcal{E}\{H\} = M_1(\rho), \tag{10}$$

$$\mathrm{var}\{H\} = M_2(\rho) - |M_1(\rho)|^2. \tag{11}$$

where M_1 and M_2 are given in Appendix B. To illustrate the results, consider a simple case: the ratio $1/(1+z)$ with z zero-mean complex normally distributed (see Fig. 2). For small values of the radius ρ the *mean square error* (MSE) is mainly due to the variance while for large values the bias dominates. A minimum of the MSE is obtained around $\rho \approx 0.5$ for reasonable values of the SNR of z. For good signal-to-noise ratios the increase for small radii cannot be shown in Fig. 2, therefore it is illustrated in Fig. 3.

The above results show that for a functional relation, by excluding the measurements where the input Fourier coefficients, X_m, are smaller than $\rho|U|$ with $0 < \rho \leq 0.5$, it is possible to obtain estimates with a finite variance. Moreover, this variance, for large values of the input SNR, corresponds to the one obtained by means of linearization (5), i.e., $\mathrm{var}\{1/(1+z)\} \approx$

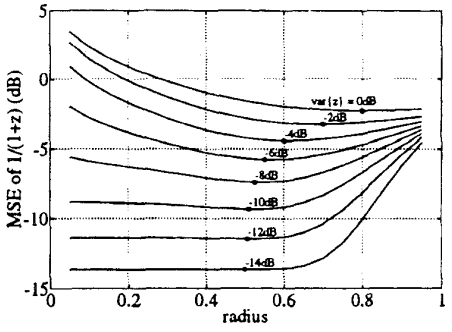

Fig. 2. MSE of $1/1+z$ versus the radius of the excluded circle around $z=-1$ for different values of the variance of z. The circles indicate the minimum MSE.

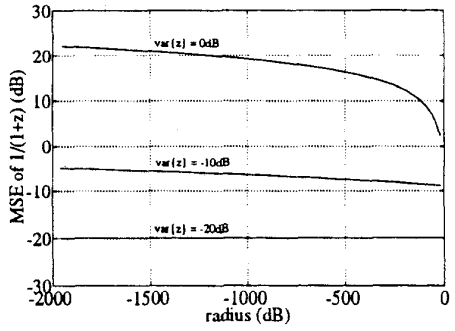

Fig. 3. MSE of $1/1+z$ versus the radius of the excluded circle around $z=-1$ for different values of the variance of z.

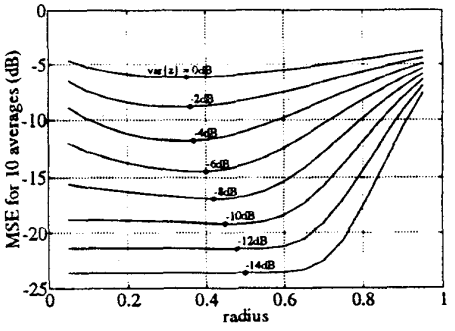

Fig. 4. MSE of $\hat{H}_{\mathrm{ARI}}^{[10]}$ versus the radius of the excluded circle around $z=-1$ for different values of the variance of z.

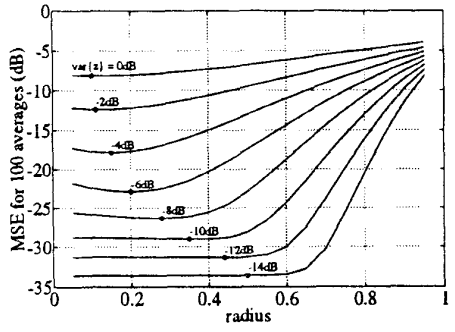

Fig. 5. MSE of $\hat{H}_{\mathrm{ARI}}^{[100]}$ versus the radius of the excluded circle around $z=-1$ for different values of the variance of z.

$\mathrm{var}\{z\}$ (see for instance Fig. 2). Thus, in practice, when taking the arithmetic mean of the ETFE's

$$\hat{H}_{\mathrm{ARI}}^{[M]} = \frac{1}{M}\sum_{m=1}^{M}\frac{Y_m}{X_m} \tag{12}$$

one needs to estimate U first, in order to be able to choose a reasonable value of ρ. Notice that the variance of the arithmetic mean of the ETFE's (12) decreases in $1/M$. The effect of this on the optimal radius is illustrated in Fig. 4 for $M=10$ and in Fig. 5 for $M=100$. One observes that there is a shift of the optimal radius to the left due to the decrease in variance. This shift is not so important for large SNR's.

When the measurements are synchronized, the sample mean of the measured input Fourier coefficients, i.e., $\hat{U} = 1/M\ \Sigma_{m=1}^{M} X_m$, can be used. Otherwise, when measuring in free-run (i.e., when no trigger signal is used) one can consider averaging the absolute values, $|X_m|$, of the delayed data records and estimate $|U|$ from these. Then, all input/output data satisfying $|X_m| < \rho|\hat{U}|$ have to be excluded from the summation (12) to minimize the MSE. Fortunately, the MSE is not sensitive to the optimal choice of $\rho|\hat{U}|$, therefore the largest value that is guaranteed to be below $0.5|U|$ can be selected.

IV. The Variance of the Logarithm of the ETFE

In Appendix A it is shown that the variance of the ETFE can be unbounded in the presence of input noise. By excluding a small region around the singularity it is possible to obtain finite variances. In this section the logarithm of the ETFE is considered: $\ln(H)$. From Appendix C it follows that the variance of $\ln(H) = \ln|H| + i\arg(H)$ is finite:

$$\mathrm{var}\{\ln(H)\} \approx \sum_{k=1}^{\infty}\frac{\sigma_\delta^{2k}\gamma\left(k+1,\dfrac{1}{\sigma_\delta^2}\right)}{k^2} \tag{13}$$

where $\gamma(\alpha,x) = \int_0^x \exp(-t)t^{\alpha-1}\,dt$ is the incomplete gamma function ([14], equation 8.350.1), and that

$$\mathrm{var}\{\ln|H|\} \approx \mathrm{var}\{\arg(H)\} \approx 0.5\ \mathrm{var}\{\ln(H)\}. \tag{14}$$

So, averaging the ETFE's in a logarithmic scale results in bounded variances, i.e., $\mathrm{var}\{\ln(Y/X)\}$ is finite. In the next section it will be shown that when at least two logarithmic values are averaged ($M \geq 2$), and the transfer function estimate is calculated as the exponent of this average,

$$\hat{H}_{\mathrm{LOG}}^{[M]} = \exp\left(\frac{1}{M}\sum_{m=1}^{M}\ln\left(\frac{Y_m}{X_m}\right)\right) \tag{15}$$

the variance of this estimate is also finite. Therefore, logarithmic averaging (or, in other words, the complex geometric mean) is preferable for the averaging of nonparametric transfer function estimates. Moreover, one can wonder if there are other functions, $g(\cdot)$, such that $\mathrm{var}\{g(Y_m/X_m)\}$ (or $\mathrm{var}\{g^{-1}(1/M\ \Sigma_{m=1}^{M} g(Y_m/X_m))\}$) is finite. The general

conditions that have to be satisfied to have finite variance are considered in the following section.

V. General Conditions for Finite Moments

The nth (absolute) moment (about the origin) of $g(Y/X)$ is given by

$$M_n = \int |g(Y/X)|^n p_{XY}(X,Y)\, d^2X\, d^2Y \qquad (16)$$

where $p_{XY}(X,Y)$ is the joint *probability density function* (PDF) of the measured I/O Fourier coefficients. Transforming (16) into polar coordinates yields

$$M_n = \int f_n(a,b,\alpha,\beta)\, da\, d\alpha\, db\, d\beta \qquad (17)$$

where $f_n = |g(e^{i(\beta-\alpha)}b/a)|^n p_{XY}(ae^{i\alpha}, be^{i\beta})\, a\, b$. To have finite moments M_n, the integrand f_n should satisfy the following conditions:

1) If a_s is a singular point of f_n, then $\lim_{a\to a_s}(a-a_s) f_n$ should equal 0. (i.e., f_n should go slower to infinity than $1/a - a_s$.)
2) As one has to integrate f_n for a going from 0 to ∞, f_n should decay faster than $1/a$ to 0 for M_n to be finite.

Similar conditions should hold for the other arguments too.

Consider, for example, the ETFE. The integrand f_n reduces to

$$f_n(a,b,\alpha,\beta) = \frac{b^{n+1}}{a^{n-1}} p_{XY}(ae^{i\alpha}, be^{i\beta}). \qquad (18)$$

Notice that $a = 0$ is a singular point of f_n for $n \geq 2$. To have a finite integral, f_n shouldn't go faster to ∞ than $1/a$ when $a \to 0$, i.e., $\lim_{a\to 0} a\, f_n$ should be equal to 0 (condition 1). This is true for $n = 1$, but not for $n = 2, 3, \cdots$, which explains why the mean value of the ETFE exists while its variance and higher-order moments are unbounded. Moreover, f_n has to decay faster than $1/a$ for $a \to \infty$ (condition 2). This condition is easily satisfied for complex normally distributed errors (due to its exponential decay). (Notice that in the case of *real-valued* normals even the mean of the ratio does not exist (see (noncentral) Cauchy distribution, [15]).) Furthermore, one can verify that *all* moments of $\ln(Y/X)$ are finite (e.g., $\lim_{a\to 0}\ a^2 \ln^n(a) = 0, n = 1, 2, \cdots$). Finally, we will show that the variance of (15) is finite for $M \geq 2$. Noticing that $\hat{H}_{\mathrm{LOG}}^{[M]}$ equals $\sqrt[M]{Y_1/X_1 \cdots Y_M/X_M}$ (i.e., the complex geometric mean) the integrand f_n with respect to $X_1 = ae^{i\alpha}$ and $Y_1 = be^{i\beta}$, for instance, becomes

$$f_n(a,b,\alpha,\beta) = \frac{b^{(n/M)+1}}{a^{(n/M)-1}} p_{X_1Y_1}(ae^{i\alpha}, be^{i\beta}). \qquad (19)$$

One notices that for $n = 1, \cdots, 2M-1$ the nth order moment of $\hat{H}_{\mathrm{LOG}}^{[M]}$ is finite (condition 1 is satisfied), while for $n \geq 2M$ the moments M_n do not exist. Thus, the variance of $\hat{H}_{\mathrm{LOG}}^{[M]}$ exists when $M \geq 2$.

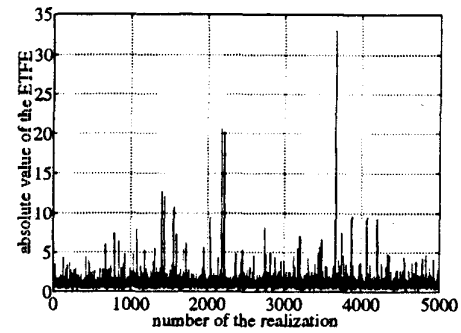

Fig. 6. 5000 realizations of the ETFE.

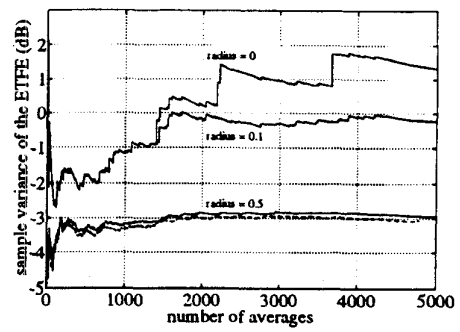

Fig. 7. Sample variance of the ETFE. Solid line: all ETFE with $|X|$ smaller than the radius ρ are set equal to 0; dashed line: all ETFE with $|X|$ smaller than the radius ρ are excluded from the summation.

VI. Simulation Results

In this section the theoretical results are verified by means of Monte-Carlo simulations. In Fig. 6 $M = 5000$ realizations of the ETFE obtained for $U = V = 1$ and $\mathrm{var}\{D\} = \mathrm{var}\{E\} = 0.25$ are depicted. A few obviously large peaks can be observed. These correspond to the cases when the denominator is very small. The sample variance for different values of the radius ρ are given in Fig. 7. In this case, the linearized variance equals 0.5 (-3 dB). For a radius of 0.1 one can show that the theoretical variance equals 0.891 (-0.5 dB) which is in good agreement with the simulation results. For $\rho = 0$, the sample variance increases without a bound.

Similar figures were plotted to check the logarithmic average. From Fig. 8 it is clear that the isolated large peaks have disappeared, so we may indeed have a population that has finite variance. The sample variance shown in Fig. 9 indeed seems to converge.

VII. Conclusions

It was shown that the variance of the ETFE is infinite for noisy input observations, even if the input noise is relatively small. This is not a well-known phenomenon. Two remedies were suggested and investigated: exclusion of a small region around the singularity of the ratio, and using logarithmic averaging (the complex geometric mean of the individual estimates). Both methods work well. This was theoretically proved, and illustrated by simulations.

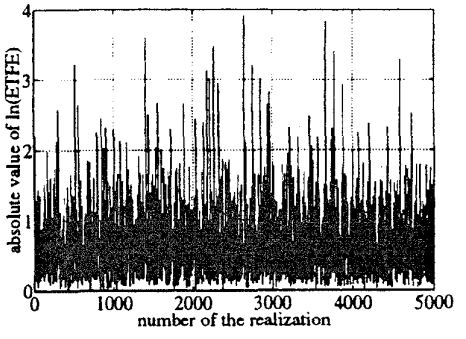

Fig. 8. 5000 realizations of ln(ETFE) using the same data as in Fig. 6.

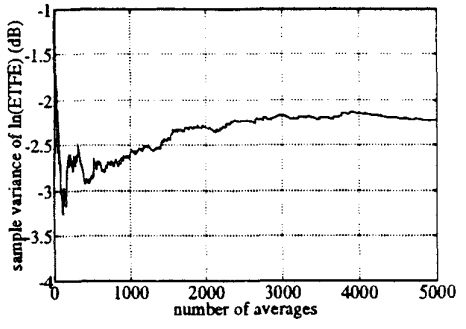

Fig. 9. Sample variance of ln(ETFE).

Appendix A
The Variance of the ETFE

In this appendix it will be shown that the variance of the ETFE is *unbounded* for a functional relationship with complex normally distributed I/O disturbances. Assuming the I/O disturbances to be independent, the joint *probability density function* (PDF) of the disturbances becomes

$$p_{DE}(D,E) = p_D(D)p_E(E) \tag{20}$$

Notice that the ETFE can be rewritten as

$$H = G\frac{1+E/V}{1+D/U} = G\frac{1+\epsilon}{1+\delta} \tag{21}$$

and that

$$\mathrm{var}\{H\} = \mathcal{E}\{|H|^2\} - |\mathcal{E}\{H\}|^2 \tag{22}$$

As $\mathcal{E}\{H\}$ is finite (see [5]), it remains to be shown that $\mathcal{E}\{|H|^2\}$ is *infinite*. To do so, the expected value of $|1/(1+\delta)|^2$ will be considered first, i.e.,

$$I_\delta = \mathcal{E}\left\{\left|\frac{1}{1+\delta}\right|^2\right\} = \int_C \left|\frac{1}{1+\delta}\right|^2 \frac{e^{-(|\delta|^2/\sigma_\delta^2)}}{\pi\sigma_\delta^2} d^2\delta \tag{23}$$

where $d^2\delta = d\mathrm{Re}(\delta)\, d\mathrm{Im}(\delta)$. Transforming (23) to polar coordinates (i.e., $\mathrm{Re}(\delta) = a\cos\alpha, \mathrm{Im}(\delta) = a\sin\alpha$) yields (see [14], equation 3.792.1 on p. 435)

$$\begin{aligned} I_\delta &= \frac{1}{\pi\sigma_\delta^2}\int_0^\infty \int_{-\pi}^{+\pi} \frac{e^{-a^2/\sigma_\delta^2}\, a\, da\, d\alpha}{1+2a\cos\alpha+a^2} \\ &= \frac{2}{\sigma_\delta^2}\int_0^\infty \frac{e^{-a^2/\sigma_\delta^2}, a\, da}{|1-a^2|} \end{aligned} \tag{24}$$

$$> \frac{e^{-1/\sigma_\delta^2}}{\sigma_\delta^2}\int_{1-\rho_u}^1 \frac{du}{1-u} = +\infty \tag{25}$$

Since $|\mathcal{E}\{H\}|^2$ in (22) is finite, one concludes that the variance of the ETFE is infinite for deterministic U in the presence of complex normally distributed input disturbances.

Appendix B
Exclusion of the Simgularity

In this appendix a small circle around the singularity point $X = 0$ will be excluded. This means that when an input Fourier coefficient is smaller than say ρ, the ETFE is set equal to zero (instead of its large value). In order to assess the effect of this operation on the bias and the variance of the ETFE, the following integrals (with respect to X) have to be evaluated:

$$M_1^X(\rho) = \int_\rho^\infty \int_{-\pi}^{+\pi} \frac{1}{ae^{i\alpha}}\, p_X(ae^{i\alpha})\, a\, da\, d\alpha \tag{26}$$

$$M_2^X(\rho) = \int_\rho^\infty \int_{-\pi}^{+\pi} \frac{1}{a^2} p_X(ae^{i\alpha})\, a\, da\, d\alpha \tag{27}$$

where

$$\begin{aligned} p_X(ae^{i\alpha}) &= \frac{e^{-(|ae^{i\alpha}-1|^2/\sigma_\delta^2)}}{\pi\sigma_\delta^2} \\ &= \frac{e^{-(1/\sigma_\delta^2)}e^{2a\cos\alpha/\sigma_\delta^2}e^{-(a^2/\sigma_\delta^2)}}{\pi\sigma_\delta^2} \end{aligned} \tag{28}$$

and $ae^{i\alpha}$ is the polar coordinates representation of $\xi = X/U = 1 + D/U$. From ([14], equations 3.915.2 and 3.915.4) one deduces that

$$\int_{-\pi}^{+\pi} e^{\mu\cos\alpha}\, d\alpha = 2\pi I_0(\mu), \tag{29}$$

$$\int_{-\pi}^{+\pi} e^{\mu\cos\alpha}\cos\alpha\, d\alpha = 2\pi I_1(\mu), \tag{30}$$

where I_i stands for the ith order Bessel function. Consequently, after integration over α, one obtains

$$M_1^X(\rho) = \frac{2e^{-(1/\sigma_\delta^2)}}{\sigma_\delta^2}\int_\rho^\infty I_1\left(\frac{2a}{\sigma_\delta^2}\right)e^{-(a^2/\sigma_\delta^2)}\, da \tag{31}$$

$$M_2^X(\rho) = \frac{2e^{-(1/\sigma_\delta^2)}}{\sigma_\delta^2}\int_\rho^\infty I_0\left(\frac{2a}{\sigma_\delta^2}\right)\frac{e^{-(a^2/\sigma_\delta^2)}}{a}\, da \tag{32}$$

Hence, assuming the input/output Fourier coefficients to be uncorrelated, the mean value and the 2nd order (absolute) moment are given by

$$M_1(\rho) = GM_1^X(\rho)M_1^Y(\rho) \tag{33}$$

$$M_2(\rho) = |G|^2 M_2^X(\rho)M_2^Y(\rho) \tag{34}$$

where

$$M_1^Y(\rho) = \frac{2e^{-(1/\sigma_\epsilon^2)}}{\sigma_\epsilon^2}\int_\rho^\infty I_1\left(\frac{2b}{\sigma_\epsilon^2}\right)e^{-(b^2/\sigma_\epsilon^2)}\, b^2\, db \tag{35}$$

$$M_2^Y(\rho) = \frac{2e^{-(1/\sigma_\epsilon^2)}}{\sigma_\epsilon^2}\int_\rho^\infty I_0\left(\frac{2b}{\sigma_\epsilon^2}\right)e^{-(a^2/\sigma_\epsilon^2)}\, b^3\, db \tag{36}$$

APPENDIX C
THE VARIANCE OF THE LOGARITHM OF THE ETFE

In this appendix it will be shown that the variance of the *complex logarithm* of the ETFE is *bounded* for a functional relationship with complex normally distributed I/O disturbances. Notice that the logarithm of the ETFE can be rewritten as (see (21))

$$\ln H = \ln G + \ln(1+\epsilon) - \ln(1+\delta). \tag{37}$$

Consider the second moment of $\ln(1+\delta)$, i.e.,

$$\mathcal{E}\{|\ln(1+\delta)|^2\} = \int_C |\ln(1+\delta)|^2 \frac{e^{-(|\delta|^2/\sigma_\delta^2)}}{\pi\sigma_\delta^2}\, d^2\delta \tag{38}$$

where $d^2\delta = d\ \mathrm{Re}(\delta)\ d\ \mathrm{Im}(\delta)$. Noticing that $\ln(z) = \ln|z| + i\arg(z)$ leads to $\mathcal{E}\{|\ln(1+\delta)|^2\} = I_\delta^a + I_\delta^\alpha$, with

$$I_\delta^a = \int_C \ln^2|1+\delta| \frac{e^{-(|\delta|^2/\sigma_\delta^2)}}{\pi\sigma_\delta^2}\, d^2\delta \tag{39}$$

$$I_\delta^\alpha = \int_C \arg^2(1+\delta) \frac{e^{-(|\delta|^2/\sigma_\delta^2)}}{\pi\sigma_\delta^2}\, d^2\delta. \tag{40}$$

Transforming (39) to polar coordinates yields

$$I_\delta^a = \int_0^\infty \int_{-\pi}^{+\pi} \ln^2(R)\, \frac{e^{-(a^2/\sigma_\delta^2)}}{4\pi\sigma_\delta^2}\, a\, da\, d\alpha \tag{41}$$

where $R = 1 + 2a\cos\alpha + a^2$. To evaluate the integral with respect to α the Parseval relation will be used:

$$\int_{-\pi}^{+\pi} x^2(\alpha)\, d\alpha = \frac{C_0^2}{2} + \sum_{k=1}^{\infty} C_k^2 + S_k^2 \tag{42}$$

where

$$C_k = \frac{1}{\sqrt{\pi}} \int_{-\pi}^{+\pi} x(\alpha)\cos(k\alpha)\, d\alpha \tag{43}$$

$$S_k = \frac{1}{\sqrt{\pi}} \int_{-\pi}^{+\pi} x(\alpha)\sin(k\alpha)\, d\alpha. \tag{44}$$

Applying (42) for $x(\alpha) = \ln(R)$ yields

$$C_0 = \begin{cases} 0, & \text{if } |a| \le 1 \\ 4\sqrt{\pi}\ \ln a, & \text{if } |a| > 1. \end{cases} \tag{45}$$

$$C_k = \begin{cases} (-1)^{k+1} 2\sqrt{\pi}\, \dfrac{a^k}{k}, & \text{if } |a| \le 1 \\ (-1)^{k+1} 2\sqrt{\pi}\, \dfrac{1}{ka^k}, & \text{if } |a| > 1 \end{cases} \tag{46}$$

$$S_k = 0 \tag{47}$$

Consequently, (39) can be written as $I_\delta^a = A_\delta^a + B_\delta^a + C_\delta^a$ where (see [14], equations 4.225.4 and 4.397.6)

$$A_\delta^a = \frac{1}{2\sigma_\delta^2} \sum_{k=1}^{\infty} \frac{1}{k^2} \int_0^1 u^k e^{-(u/\sigma_\delta^2)}\, du \tag{48}$$

$$B_\delta^a = \frac{1}{4\sigma_\delta^2} \int_1^\infty \ln^2(u) e^{-(u/\sigma_\delta^2)}\, du \tag{49}$$

$$C_\delta^a = \frac{1}{2\sigma_\delta^2} \sum_{k=1}^{\infty} \frac{1}{k^2} \int_1^\infty \frac{1}{u^k} e^{-(u/\sigma_\delta^2)}\, du. \tag{50}$$

The main contribution to I_δ^a is given by A_δ^a which reduces to

$$A_\delta^a = \sum_{k=1}^{\infty} \frac{\sigma_\delta^{2k}\, \gamma\left(k+1, \dfrac{1}{\sigma_\delta^2}\right)}{2k^2} \tag{51}$$

where $\gamma(\alpha, x) = \int_0^x \exp(-t)t^{\alpha-1}\, dt$ is the incomplete gamma function ([14], equation 8.350.1). Before evaluating the remaining terms (i.e., B_δ^a and C_δ^a) the integral I_δ^α (see (40)) will be considered. The main contribution of (40) (i.e., the integral for a going from 0 to 1) can be formulated as

$$A_\delta^\alpha = \int_0^1 \int_{-\pi}^{+\pi} \arctan^2(S)\, \frac{e^{-(a^2/\sigma_\delta^2)}}{\pi\sigma_\delta^2}\, a\, da\, d\alpha \tag{52}$$

where $S = a\sin\alpha/(1 + a\cos\alpha)$. Applying once again (42) but this time for $x(\alpha) = \arctan(S)$ yields (see [14], equation 4.575.1)

$$C_0 = 0 \tag{53}$$

$$C_k = 0 \tag{54}$$

$$S_k = \sqrt{\pi}\, \frac{a^k}{k}, \quad \text{if } |a| \le 1. \tag{55}$$

Consequently, $A_\delta^\alpha = A_\delta^a$, so that the main contributions to I_δ^a and I_δ^α are equal. Noticing that $\ln^2(u) \le u^2$ and $1/u^2 < 1$ for $u \ge 1$, the following upper bounds can be derived for (49) and (50)

$$B_\delta^a < \frac{\sigma_\delta^4 \left[2 - \gamma\left(3, \dfrac{1}{\sigma_\delta^2}\right)\right]}{4} \tag{56}$$

$$C_\delta^a < e^{-(1/\sigma_\delta^2)}. \tag{57}$$

($\Sigma_{k=1}^\infty\ 1/k^2 = 1.644\,934\ldots$). The remaining term of (40), B_δ^α, (i.e., the integral for a going from 1 to ∞) is bounded by ($\arg(1+\delta) \le \arg(\delta)$)

$$B_\delta^\alpha < \pi^3 \sigma_\delta^2\, e^{-(1/\sigma_\delta^2)}. \tag{58}$$

REFERENCES

[1] M. Kendall and A. Stuart, *Inference and Relationship*, vol. 2 of *The Advanced Theory of Statistics*. London: Charles Griffin, London, 1979, 4th ed., vol. 2.

[2] L. J. Gleser, "Estimation in a multivariable 'errors-in-variables regression model: Large sample results," *Ann. Stat.*, vol. 9, no. 1, pp. 24–44, 1981.

[3] W. A. Fuller, *Measurement Error Models*. New York: Wiley, 1987.

[4] B. D. O. Anderson, "Identification of scalar errors-in-variables models with dynamics, *Automatica*, vol. 21, no. 6, pp. 709–716, 1985.

[5] P. Guillaume, R. Pintelon, and J. Schoukens, "Nonparametric frequency response function estimators based on nonlinear averaging techniques," *IEEE Trans. Instrum. Meas.*, vol. 41, no. 6, pp. 739–747, Dec. 1992.

[6] A. Papoulis, *Probability, Random Variables, and Stochastic Processes*. New York: McGraw-Hill, 1981.

[7] L. Ljung, *System Identification: Theory for the User*. Englewood Cliffs, NJ: Prentice Hall, 1987.

[8] J. Schoukens and R. Pintelon, *Identification of Linear Systems: A Practical Guideline to Accurate Modeling*. Oxford: Pergamon, 1991.

[9] D. R. Brillinger, *Time Series: Data Analysis and Theory*. New York: McGraw-Hill, expanded edition, 1981.

[10] P. M. T. Broersen, "A comparison of transfer function estimators," in *Proc. 10th IEEE Instrumentation and Measurement Technology Conf.* vol. 3, pp. 1377–1380, Hamamatsu, May 10–12 1994.

[11] P. Billingsley, *Probability and Measure*, 2d ed. New York: Wiley, 1985.

[12] P. Guillaume, *Identification of Multi-Input Multi-Output Systems Using Frequency-Domain Models,* Ph.D. thesis, Vrije Universiteit Brussel, Belgium, June 1992.
[13] P. H. Sydenham, Ed., *Handbook of Measurement Science.* New York: Wiley, 1982, vol. 1, ch. 8.
[14] I. S. Gradshteyn and I. M. Ryzhik, *Table of Integrals, Series, and Products.* New York: Academic, corrected and enlarged edition, 1980.
[15] A. Stuart and J. K. Ord, *Distribution Theory,* vol 1 of *Kendall's Advanced Theory of Statistics,* 5th ed. London: Charles Griffin, 1987.

Patrick Guillaume (S'86–M'87), for a photograph and biography, see p. 11 of the February 1996 issue of this TRANSACTIONS.

István Kollár, for a photograph and biography, see this issue, p. 361.

Rik Pintelon, for a photograph and biography, see p. 11 of the February 1996 issue of this TRANSACTIONS.